Synthesis and Characterization of PVP/LiCoO$_2$ Nanofibers by Electrospinning Route

Lin-Jer Chen,[1] Jiunn-Der Liao,[1] Yu-Ju Chuang,[1] Kuo-Chin Hsu,[1] Yi-Fang Chiang,[2] Yaw-Shyan Fu[3]

[1]Department of Materials Science and Engineering, National Cheng Kung University, Tainan 701, Taiwan
[2]Institute of Electro-Optical Science and Engineering, National Cheng Kung University, Tainan 701, Taiwan
[3]Department of Greenergy Technology, National University of Tainan, Tainan 701, Taiwan

ABSTRACT: We have successfully prepared PVP/LiCoO$_2$ nanofibers using an electrospinning route. These fibers were composed of very small crystalline grains uniformly linked with an average size. After annealing of the above precursor fibers at 700°C for 12 h, LiCoO$_2$ nanofibers with 95 nm in diameter were composed of crystalline nanoparticles were successfully obtained. The morphology, crystal structure, and particle size of fibers has been characterized by scanning electron microscopy (SEM), energy dispersive spectrometer (EDS), X-ray diffraction (XRD). The viscosities of solutions were measured with a LVDV Brookfield viscometer. Experimental results showed that the LiCoO$_2$ with good crystalline and uniform diameter were obtained. © 2011 Wiley Periodicals, Inc. J Appl Polym Sci 121: 154–160, 2011

Key words: annealing; composites; crystallization; nanofiber; synthesis

INTRODUCTION

LiCoO$_2$ is an important material in the last a few years in the application as a cathode material for the lithium secondary batteries. To increase capacity of a LiCoO$_2$ electrode, it is necessary to reduce particle size because the surface/volume ratio increases.[1] There are many methods for producing nanofibers, such as gas-phase reaction,[2] gas-liquid-solid,[3] solution-liquid-solid process,[4] and solvothermal method.[5] However, most methods require high temperature and long-time reaction,[6] which are not only long-time, but also difficult to control the process of fiber formation.

Of these, the synthesis of LiCoO$_2$ is carried out by the solid-state reaction process involving mechanical mixing of lithium and cobalt salts followed by firing for high temperature and long time. This process inevitably leads to the abnormal grain growth and poor control of stoichiometry. The electrospinning route solves the compound of cobalt and lithium into a liquid, and then LiCoO$_2$ nanofibers can be produced after calcinations. This method can obtain a homogeneous precursor, and form LiCoO$_2$ under low calcinations temperatures. Hence, it can decrease the reaction time, and the chemical stoichiometry of reactant is easily controllable. Nishizawa et al.[7] proved that the charge-discharge performance can be improved if LiMn$_2$O$_4$ is made into nanotubes. Gu et al.[8] compared the properties of fibers and particles of LiCoO$_2$, and pointed out that the nanofiber structure of LiCoO$_2$ could improve energy density and efficacy.

Electrospinning is a process to manufacture nanofibers, to manufacture various materials, such as polymeric materials, composite materials, and ceramic materials. It can adjust the fiber diameters in a range of 10 nm to 10 μm, thus can control the surface texture, compositions, and collection and layout of fibers. It can also produce hollow nanotubes.[9,10] Although the electrospinning process is simple, there are many variables affecting the fiber formation, including solution viscosity, electrostatic charge density of solution, solution conductivity, solution surface tension, electric field strength, solution flow rate, and distance to collector.[11–20]

Thus, better efficiency, longer life, and higher stability of lithium ion battery during the charge-discharge process, producing LiCoO$_2$ nanofibers is an important factor. The novel electrospinning process adopted in this experiment can remedy these defects, and quickly and conveniently obtain LiCoO$_2$ fibers with large surface area and small pores.[21] Polyvinylpyrrolidone often employed due to its low toxicity, high aqueous solubility, and extensively
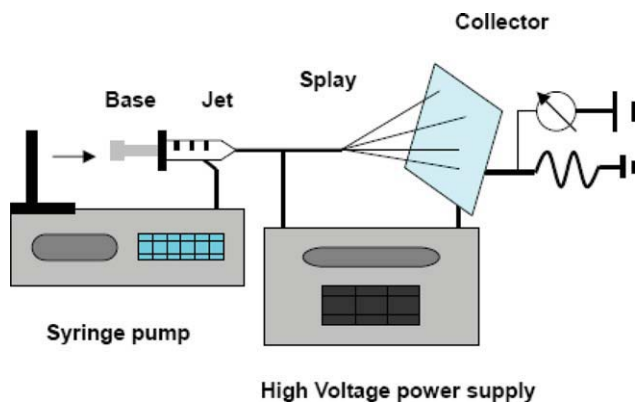
Figure 1 Schematic diagram of electrospinning device. [Color figure can be viewed in the online issue, which is available at wileyonlinelibrary.com.]

used as a stabilizer and structure-directing agent in nanotechnology owing to its excellent adsorption ability.[22] In the present work, the preparation of LiCoO$_2$ nanofibers with 95 nm in diameter by the polyvinylpyrrolidone assisted electrospinning technique is introduced.

EXPERIMENTAL

Materials

Cobalt acetate [Co (CH$_3$COO)$_3$·4H$_2$O] (WAKO CHE. Co.), lithium acetate [Li (CH$_3$COO). 2H$_2$O] (OSAKA Co.), methyl alcohol (OSAKA Co.), acetic acid (OSAKA Co.), polyvinylpyrrolidone (ACROS Co.).

Preparation of precursor of LiCoO$_2$

The precursor was prepared as follows: cobalt acetate (0.001 mol) and lithium acetate (0.001 mol) into different beakers, which were dissolved in 2 mL methanol with magnetically stirred at room temperature for 2 h to obtain homogenous solution, respectively. The whole mixture was stirred for 2 h at
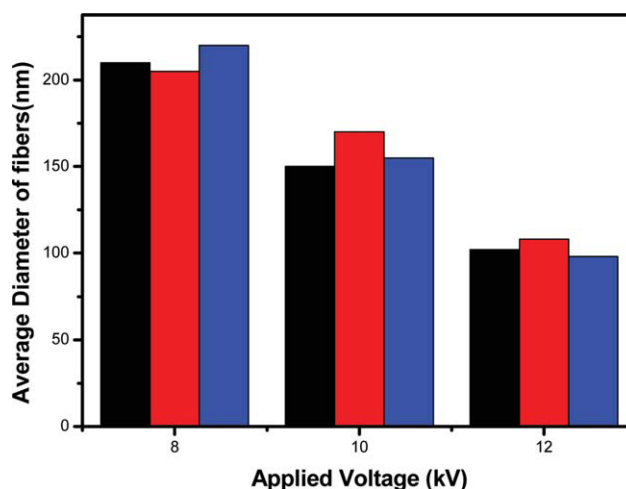

Figure 3 LiCoO$_2$ nanofibers average diameter on voltages by annealing at 700°C for 12 h. [Color figure can be viewed in the online issue, which is available at wileyonlinelibrary.com.]

room temperature, and finally obtain 0.25M precursor of LiCoO$_2$.

Preparation of the LiCoO$_2$ nanofibers

The preparation process is as follows: 0.06 g PVP into a beaker, and add 1 mL methanol for 10 min by ultrasonic oscillator. A mixture of LiCoO$_2$ precursor and PVP solution with magnetically stirred at room temperature for 2 h to obtain homogenous LiCoO$_2$/PVP solution. The schematic setup of the electrospinning route used in the study was shown in Figure 1. In electrospinning of polymer solutions, the fiber formation process can be characterized by the formation and thinning of the liquid jet to the solidification and deposition of fibers on the collecting target. A stainless steel electrode was connected to a high voltage power supply (You-Shang Technical Corp.), which can generate DC voltage up to 30 kV. The supplied voltages between the tip and collector were set at 8 kV with a tip-to-collector
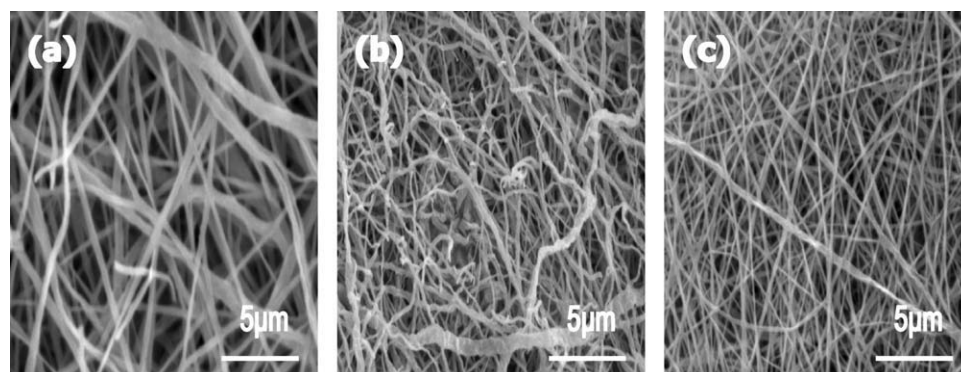

Figure 2 SEM images of LiCoO$_2$ fibers (bar 5 μm) electrospinning from various voltages are (a) 8 kV, (b) 10 kV, and (c) 12 kV by annealing at 700°C for 12 h.
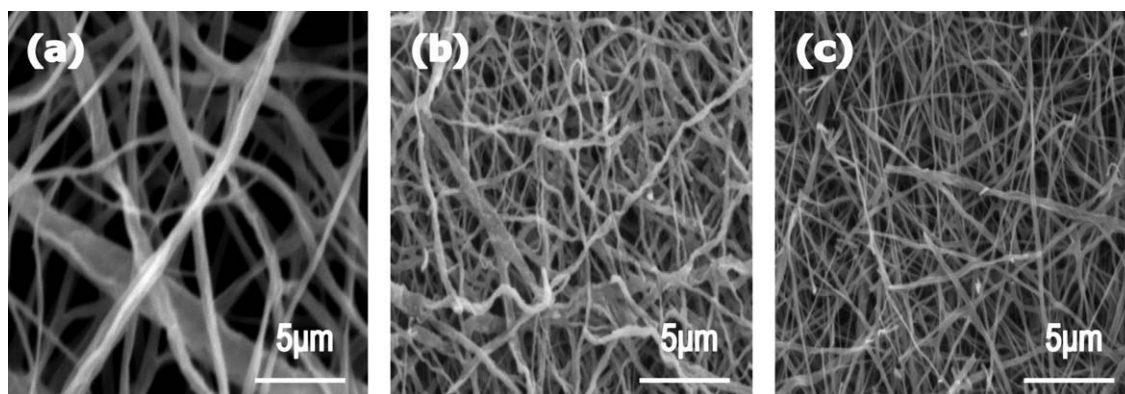
Figure 4 SEM images of LiCoO$_2$ fibers (bar 5 μm) electrospinning (12 kV) various annealing temperature at (a) 300°C, (b) 500°C, and (c) 700°C for 12 h.

distance of 5 cm. The applied voltage first overcomes the liquid surface tension to form a jet, which then bend, and spiral into a larger looping path as the jet thins into finer fibers and solidifies. Homogeneous solutions of LiCoO$_2$ were prepared and added PVP with gentle magnetic stirring at ambient temperature for 1 to 2 h. The solutions were prepared and used immediately for electrospinning. Finally LiCoO$_2$ nanofibers can be obtained for calcinations at 700°C for 12 h. Change the voltage to 10 kV and 12 kV, respectively, and repeat the steps described above.

Morphologies of LiCoO$_2$ nanofibers

The as-prepared samples were characterized by X-ray diffraction (XRD), scanning electron microscopy (SEM), respectively, XRD was carried out on a D/MAX-500 X-ray powder diffraction with Cu Kα radiation (λ = 1.5418 E). The scanning rate of 0.02 s^{-1} was applied to record the patterns in the two Theta range of 10 to 80°. The X-ray energy dispersive spectroscopy (EDS) was recorded on an EX220, HORIVA spectroscopy, which was attached to the SEM for composition analysis. The viscosities of solutions were measured with a LVDV Brookfield viscometer.

RESULTS AND DISCUSSION

Morphologies structure of electrospinning PVP/LiCoO$_2$ fiber formation

In our work, a sol held by its surface tension at the end of a capillary tube was subjected to an electric field and the charge was induced on the liquid surface by the applied voltage, causing a force directly opposite to the surface tension. As the intensity of the electric field was high enough, a charged sol jet was ejected from the spinneret to form the gel fibers falling on the collector. Figure 2(a–c) shows SEM micrographs of the electrospinning PVP/LiCoO$_2$

fibers at three different applied voltages, 8 kV, 10 kV, and 12 kV. The electrospinning PVP/LiCoO$_2$ fibers obtained at 10 kV are, on the whole, thicker than those obtained at 12 kV. When the voltage is increased to the threshold value, a droplet of hybrid solution at the tip is deformed into a conical shape known as Taylor cone. In this work, charge or dipole orientation will be formed at the interface between air and the droplet. With increasing the voltages applied to the solution in a certain range, the electrostatic force is larger than the surface tension, and the fibers become thinner when the other parameters remain unchanged. The results are summarized in Figure 3. It is observed that the diameter distribution of the PVP/LiCoO$_2$ fibers is shifted to the smaller size as the applied voltage increases. This trend of reduction in size with the applied voltage has been
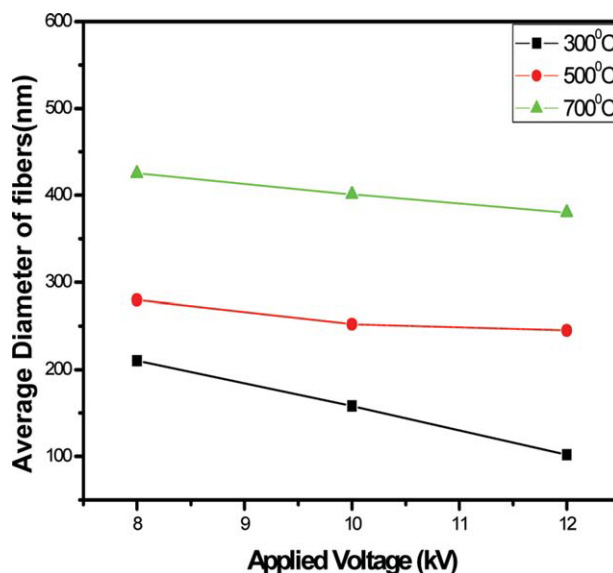

Figure 5 The changes of the average diameters of LiCoO$_2$ fibers between voltage and annealing temperature. [Color figure can be viewed in the online issue, which is available at wileyonlinelibrary.com.]
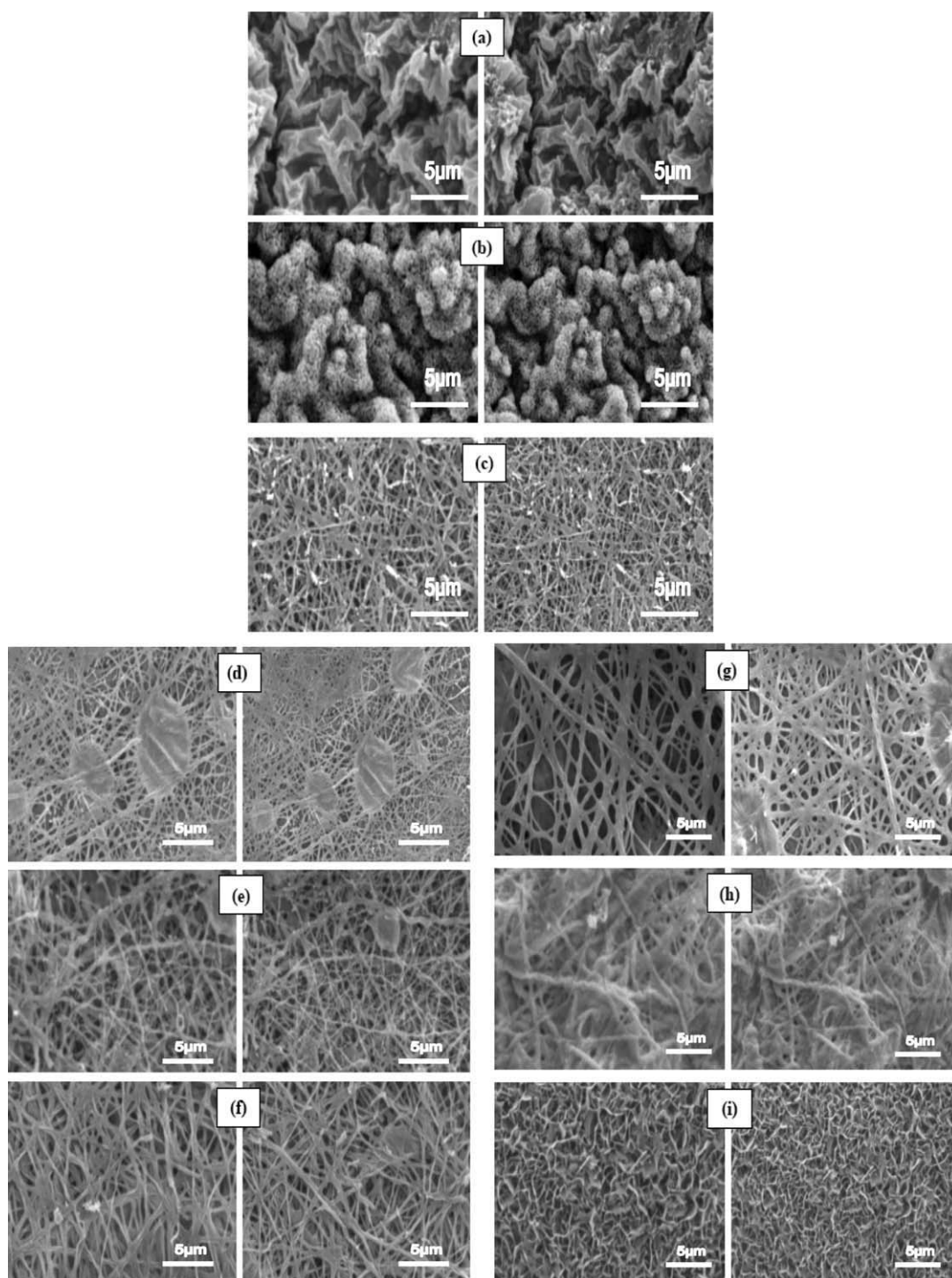
Figure 6 SEM images of LiCoO$_2$ fibers (bar 5 μm) electrospinning (12 kV) various viscosity are (a) 13.8 cp, (b) 15.9 cp, (c) 30.9 cp, (d) 35.6 cp, (e)40.4 cp, (f) 66 cp, (g) 75.9 cp (h) 103.2 cp, (i) 137.2 cp by annealing at 700°C for 12 h.

reported in various electrospinning organic fibers.[23] The most population is in the range of 90 to 220 nm for the silica fibers synthesized at 8-12 kV.

Figure 4 shows SEM micrographs of the LiCoO$_2$ fibers electrospinning (12 kV) at various annealing temperature, (a) 300°C, (b) 500°C, and (c) 700°C for 12 h, respectively (Fig. 5). The fibers obtained after annealing at 300°C and 500°C exhibited shrinkages and diameters were reduced due to the decomposition of PVP and the removal of CH$_3$COO group of cobalt acetate and lithium acetate molecules. After annealing at 800°C [Fig. 4(c)], the diameters of the fibers became smaller. It was thought to be due to the complete removal of organic molecules and the
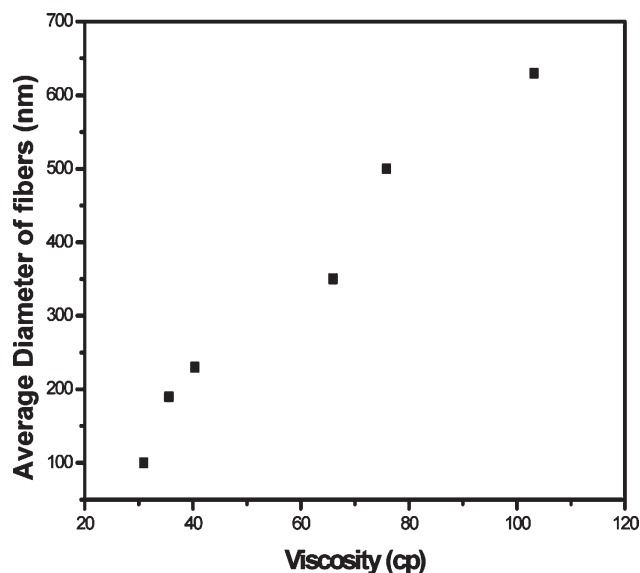
Figure 7 LiCoO$_2$ nanofibers size on viscosity by annealing at 700°C for 12 h.

development of cobalt oxide and lithium oxide crystalline.[24,25]

To illustrate the effect of parameters of solutions on the morphology and viscosity of LiCoO$_2$ nanofibers by annealing at 700°C for 12 h were examined as shown in Figure 6. The viscosities of solutions were measured with a LVDV Brookfield viscometer. Figure 6(a–i) shows SEM micrographs of the electrospinning LiCoO$_2$ fibers at various viscosity, 13.8 cp, 15.9 cp, 30.9 cp, 35.6 cp, 40.4 cp, 66 cp, 75.9 cp, 103.2 cp, and 137.2 cp, respectively. When the viscosity increased, the diameter of LiCoO$_2$ fibers increased, and bead-on-string structures appeared. On the other hand, when the viscosity further increased, the beads on fibers decreased. The results showed that high viscosity preferred electrospinning. LiCoO$_2$ nanofibers form within a range of viscosity between 30 and 100cp. It is lower than 30 cp, thread cannot be drawn to concentrate the particles. It is greater than 100 cp, the fiber morphology becomes a belt. Fong et al.[11] pointed out that, the greater the viscosity, the easier the fibers form with a larger diameter. The viscosity in the solution tends to increase the average diameter of fibers (Fig. 7). The diameter of nanofibers is in the range of 95 ± 5 nm, 185 ± 5 nm, 225 ± 5 nm, 345 ± 5 nm, 495 ± 5 nm, and 625 ± 5 nm with various viscosity. One hundred LiCoO$_2$ fibers were selected from 10 spots of 60 × 60 μm^2 to measure the distribution of the diameters. The average fiber sizes increased with increasing solution viscosity from above solution series. The high conductivity solvent is helpful to the ion diffusion and reduces resistance. The high viscosity solvent can cause the diffusion of ions not to be easy, to reduce the conductivity.[26]

Crystalline structure of electrospinning LiCoO$_2$ nanofiber

Figure 8 shows the XRD patterns of PVP/LiCoO$_2$ composites fibers by electrospinning process at the various applied voltage (8 kV, 10 kV, and 12 kV) after annealing by (a) 300°C, (b) 500°C, and (c) 700°C for 12 h, respectively. From the XRD spectra, ten diffraction peaks corresponding to (003), (101), (006), (012), (104), (105), (107), (108), (110), and (113), respectively, can be observed.[27–30] All of the diffraction peaks can be indexed as a hexagonal phase of LiCoO$_2$ (JCPDS 44-145), which implies pure LiCoO$_2$ has been synthesized. However, with the raise of the annealing temperature, the crystallinity of the fibers increased and the crystal structure was in good agreement with the hexagonal LiCoO$_2$. The result is a completely crystalline structure in the LiCoO$_2$ nanofibers formed with the addition of PVP to the electrospinning step. The (full width at half-maximum (fwhm) values of the PVP/LiCoO$_2$ nanofibers are similar size calculated by Scherrer equation ($D = K\lambda/$ ($\beta \cos \theta$); $K = 0.89$, $\lambda = 0.15418$ nm, $\beta = $ fwhm, $\theta = $ diffraction angle).

The morphologies of the LiCoO$_2$ nanofibers were characterized by transmission electron microscopy (TEM) observation on an H-800 with an accelerating voltage of 160 kV. Figure 9 show TEM micrographs of LiCoO$_2$ nanofibers by electrospinning at 12 kV after annealing. One can see exclusively fiber-like morphology of LiCoO$_2$. However, it can be clearly observed that the fiber-like nanostructures with the diameters of LiCoO$_2$ nanofibers about 95 nm and lengths from hundreds of nanometers to several
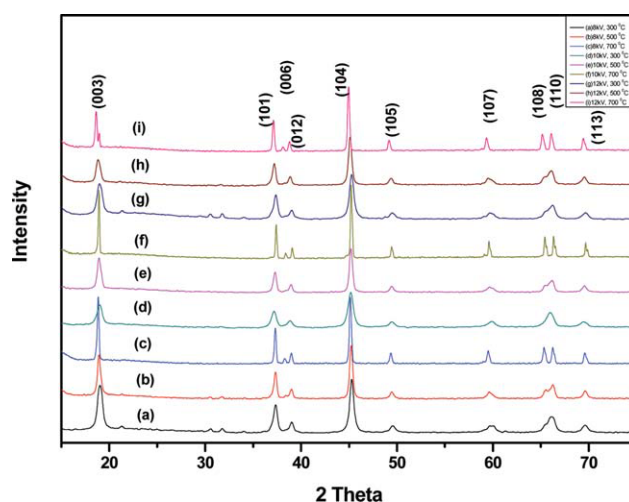

Figure 8 X-ray diffraction patterns for LiCoO$_2$ fibers electrospinning by annealing at (a) 300°C (8 kV), (b) 500°C (8 kV), (c) 700°C (8 kV), (d) 300°C (10 kV), (e) 500°C (10 kV), (f) 700°C (10 kV), (g) 300°C (12 kV), (h) 500°C (12 kV), and (i) 700°C (12 kV) for 12 h. [Color figure can be viewed in the online issue, which is available at wileyonlinelibrary.com.]
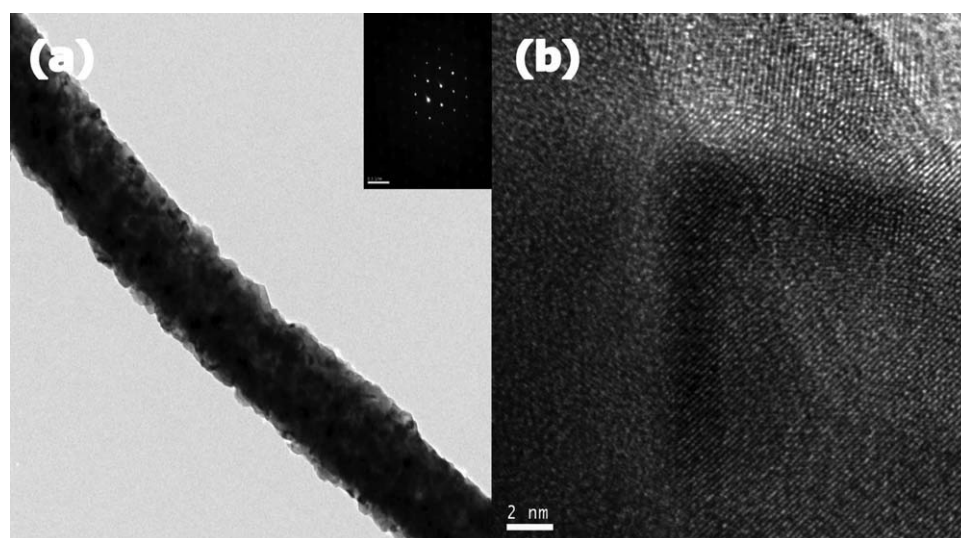
Figure 9 TEM images (a) of as-synthesized LiCoO$_2$ nanostructures and its SAED pattern (inset), (b) high-resolution TEM of fiber-like LiCoO$_2$ nanostructures.

micrometers. By changing the reaction concentrations, tip-to-collector distance, viscosity and applied voltage, the nanofibers size can be easily controlled. The crystallographic planes between adjacent particles match very well, and no amorphous impurities are observed from the HRTEM images.

Based on the above results, a potential mechanism is presented. With the interaction of LiCoO$_2$ and PVP as capping agent, the PVP molecules are assembled on the surface of LiCoO$_2$, and LiCoO$_2$ nanoparticles are partly covered by PVP long chains. There also exists interaction between LiCoO$_2$ nanoparticles because of the high Gibbs' surface free energy of the small sized LiCoO$_2$. The two competitive interactions induce larger LiCoO$_2$ and PVP cluster with different diameters. And the surface defects are partly passivated by PVP molecules. With the increase of the reaction viscosity, more LiCoO$_2$ nanoparticles with low aggregation were extracted. Then the dispersion of the LiCoO$_2$ and PVP clusters is narrower, and the passivation is more effective.

CONCLUSIONS

In this work, electrospinning LiCoO$_2$ nanofibers are investigated. When the voltage is larger, the electric field strength increases. The voltage is set as 12 kV, and nanofibers with a diameter of 95 nm can be obtained. As the annealing temperature rises, the diameter of the LiCoO$_2$ nanofibers decreases. Nanofibers with a diameter of 95 nm can be produced by the annealing temperature at 700°C for 12 h. Fibers form within a range between 30 and 100 cp. It is lower than 30 cp, thread cannot be drawn to concentrate the particles, and it is greater than 100 cp, the fiber morphology becomes a belt. This work finds

that nanofibers, with a diameter smaller than 100 nm, can be made when the viscosity is 30.9 cp. As the voltage becomes greater, the smaller fiber diameter is conducive to the crystallization of LiCoO$_2$, and the diffraction intensity of the X-ray increases. Crystallographic planes between the adjacent particles in LiCoO$_2$ fibers matched well to reduce the surface energy, which made for more lithium cations insertion and faster solid-state diffusion, greatly increasing the performance of batteries.

References

1. Miyayama, M.; Suzuki, S. Mater Stage 2003, 3, 37.
2. Levitt, A. P., Ed. Whisker Technology; Wiley-Interscience: New York, 1970.
3. Wagner, R. S.; Ellis, W. C. Appl Phys Lett 1964, 4, 89.
4. Trentler, T. J; Hickman, K. M.; Geol, S. C.; Viano, A. M.; Gibbons, P. C.; Buhro, W. E. Science 1995, 270, 1791.
5. Health, J. R.; LeGoues, F. K. Chem Phys Lett 1993, 208, 263.
6. Subramanian, V.; Chen, C. L.; Chou, H. S.; Fey, G. T. K. J Mater Chem 2001, 11, 3348.
7. Nishizawa, M.; Mukai, K.; Kuwabata, S.; Martin, C. R.; Yoneyama, H. J Electrochem Soc 1923 1997, 144.
8. Gu, Y.; Chen, D.; Jiao, X. J Phys Chem B 2005, 109, 17901.
9. Wang, X.; Drew, C.; Lee, S. H.; Senecal, K. J.; Kumar, J.; Samuelson, L. A. Nano Lett 2002, 2, 1273.
10. McCann, J. T.; Li, D.; Xia, Y. J Mater Chem 2005, 15, 735.
11. Fong, H.; Chun, I.; Reneker, D. H. Polymer 1999, 40, 4585.
12. Gupta, P.; Elkins, C.; Long, T. E.; Wilkes, G. L. Polymer 2005, 46, 4799.
13. Chen, L. J.; Liao, J. D.; Lin, S. J.; Chuang, Y. J.; Fu, Y. S. Polymer 2009, 50, 3516.
14. Kim, B.; Park, H.; Lee, S. H. Mater Lett 2005, 59, 829.
15. Son, W. K.; Youk, J. H.; Lee, T. S.; Park, W. H. Mater Lett 2005, 59, 1571.
16. Demir, M. M.; Yilgor, I.; Yilgor, E.; Erman, B. Polymer 2002, 43, 3303.
17. Lu, C.; Chen, P.; Li, J.; Zhang, Y. Polymer 2006, 47, 915.
18. Deitzel, J. M.; Kleinmeyer, J.; Harris, D.; Tan, N. C. B. Polymer 2001, 42, 261.

19. Kuo, J. C.; Lee, S. C.; Hsu, K. C.; Liu, S. J.; Chou, B. Y.; Fu, Y. S. Mater Lett 2008, 62, 4594.
20. Li, D.; Xia, Y. Nano Lett 2003, 3, 555.
21. Gu, Y.; Chen, D.; Jiao, X. J Phys Chem B 2005, 109, 17901.
22. Zhang, J.; Liu, J.; Wang, S.; Zhan, P.; Wang, Z.; Ming, N.; Adv Funct Mater 2004, 14, 1089.
23. Lee, S. G.; Choi, S. S.; Joo, C. W. J Korean Fiber Soc 2002, 39, 1.
24. Quinlan, F. T.; Vidu, R.; Predoana, L.; Zaharescu, M.; Gartner, M.; Groza, J.; Stroeve, P. Ind Eng Chem Res 2004, 43, 2468.
25. Ding, N.; Ge, X. W.; Chen, C. H. Mater Res Bull 2005, 40, 1451.
26. Ruenraroengsak, P.; Florence, A. T. Int J Pharm 2005, 298, 361.
27. Lundblad, A.; Bergman, B. Solid State Ionics 1997, 96, 173.
28. Ohuzuku, T.; Komori, H.; Nagayama, M.; Sawai, K.; Hirai, T. J Ceram Soc Jpn 1992, 100, 346.
29. Shao, C.; Yu, N.; Liu, Y.; Mu, R. J Phys Chem Solids 2006, 67, 1423.
30. Predoană, L.; Bar&acaronu, A.; Zaharescu, M.; Vassilchina, H.; Velinova, N.; Banov, B.; Momchilov, A. J Eur Ceram Soc 2007, 27, 1137.